



**E-ISSN: 2687-6167**

**Number 58, September 2024**

**RESEARCH ARTICLE**

Receive Date: 19.07.2024

Accepted Date: 06.09.2024

# Microstrip Patch Antenna Design for 5G and Beyond Wireless Communication Systems

Bahar BARISER<sup>a</sup>, Inci UMAKOGLU<sup>b,\*</sup>, Mustafa NAMDAR<sup>c</sup>, Arif BASGUMUS<sup>d</sup>

<sup>a</sup>Kutahya Dumlupınar University, Department of Electrical and Electronics Engineering, 43100, Kutahya, Turkey  
ORCID: 0000-0002-2173-7314

<sup>b</sup>Kutahya Dumlupınar University, Department of Electrical and Electronics Engineering, 43100, Kutahya, Turkey  
ORCID: 0000-0002-2786-5421

<sup>c</sup>Kutahya Dumlupınar University, Department of Electrical and Electronics Engineering, 43100, Kutahya, Turkey  
ORCID: 0000-0002-3522-4608

<sup>d</sup>Bursa Uludag University, Department of Electrical and Electronics Engineering, 16059, Bursa, Turkey,  
ORCID: 0000-0002-0611-3220

## Abstract

This paper gives a theoretical evaluation on how feeder lengths are appropriate for distinct conductor materials using rectangular microstrip patch antenna shape with the help of finite integration techniques (FIT). In this study, the ground surface width is 5.6mm and the ground surface length is 4.65 mm for the rectangular microstrip patch antenna. The length of the patch is 3.44 mm while the patch width is 4.40 mm. The substrate thickness is at 0.20 mm, the patch thickness is 0.035 mm the additional inner feed length is 1.05 mm and the microstrip line feed width is 0.6 mm. Antenna of rectangular microstrip patch type has been designed to work in the 20 – 36 frequency band and working frequency of the proposed antenna is 28 GHz. Compared to the use of a single conductor on the surface of the designed patch antenna, three different conductor materials-copper, gold, and aluminum-were applied to the patch surface of the antenna. The return loss (S11), voltage standing wave ratio (VSWR), bandwidth (BW), directivity and gain of the microstrip antenna parameters are studied using finite integration method Computer Simulation Technology (CST) based on nine different feed lengths in microstrip antenna design. When analyzing the feature of the simulation, the optimal S11 can be observed at the 28 resonant frequencies in the copper conductor. According to the analysis results, for copper conductor the best S11 was obtained at a resonant frequency of 28.03 GHz. The value of S11 is -31.19 dB and the BW value is 968 MHz. For the gold conductor the high return loss is achieved using the at the resonated frequency of 28.01 GHz. S11 value is -32 dB and the BW value is 972 MHz Aluminum conductor has the highest value of S11 with a resonant frequency of 28.01 GHz as shown in -33.29 dB and BW value is 976 MHz. Unsurprisingly, the characterization of the conductor deposition on each structure shows that aluminum conductor yielded the best S11 among all the conductor types. The VSWR is equal to 1.05 for copper conductor at resonant frequency of 28.03 GHz, 1.05 at gold conductor at a resonant frequency of 28.01 and 1.04 for aluminum conductor at a resonant frequency of 28.01 GHz. The maximum directivity values that have been attained in the three-dimensional (3D) representation of the copper conductor, gold and aluminum conductor antennas are nearly 6.99

dBi, respectively. The maximum values of the gain are obtained for the 3D representation of copper, gold and aluminum conductor antennas are 6.61, 6.60 and 6.58 dBi, respectively.

© 2023 DPU All rights reserved.

*Keywords:* 5G; Return Loss; VSWR; Gain; Directivity; CST Suite; Microstrip Patch Antenna.

## 1. Introduction

Wireless communication is a technology employed for transmitting information or data, typically through the use of electromagnetic signals [1]. Currently, wireless communication is one of the rapidly growing and influential sectors of human life and its usage is expanding [2]. Fifth generation (5G) elevates the wireless communication network in terms of its features which include high speed communications, faster data transfer, low delay or latency, and dependable connections [3].

The impact of the progressive development of wireless communication has been illustrated by introducing a new, unique approach to both improve communication reliability and the utilization of the NOMA system with the help of UAV assistance [4]. Studying the outcomes of the radio wave signal transmission scheme called the orthogonal time frequency space non-orthogonal multiple access (OTFS-NOMA) in highly mobile users for 5G wireless communication and analyzing its effects on the reliability and effectiveness of mobility-based programs has brought into the light one of the highly significant wireless application zones for 5G [5, 6]. Cited in the article are the fairly appealing findings in ergodic capacity estimation with artificial neural networks in conjunction to underscore the role of innovation in CNS for reliability [7]. Specifically, this survey investigates the 5G wireless communication by assessing the bit error rate (BER) of downlink NOMA systems. Regarding reliability and efficiency, this analysis elucidated the imperative role played by the 5G wireless communication systems [8]. In this way, through the analysis of previous studies, it can be concluded that microstrip antennas have the potential to fulfill the demands of 5G communication systems [9]. From examining the functions of microstrip antennas and from the assessments of the capability of microstrip antennas to meet the demands of the 5G application, an efficient microstrip antenna design with wide bandwidth was proposed [10]. Patch antennas are also known as microstrip antennas; they are becoming more prevalent in almost all wireless communication applications including space communications [11]. With the increasing technology in communication engineering, there is a rise in the complication of the shape of antennas which the analytical methods cannot offer a full explanation; thus, computational electromagnetic models are used to solve them fully. This reveals the general situation with the antenna structures and field radiation that make it hardly possible to obtain a full solution of the antenna problems using solely the analytical methods it is necessary to apply the computational electromagnetic models (CEM) in addition [12]. This paper has shown that finite difference method, the finite element method (FEM) and the integral equations method used to solve Maxwell's equations are important numerical methods that can be employed when handling these equations. These methods involve using Maxwell's equations to recalculate the electric and magnetic fields within a body confined by a set of physical boundary conditions. This leads us to the core of this mathematical formulation: Maxwell's equations are at the heart of this description. These equations make the foundation of electricity and magnetism which are composed of four laws [13]. Finite integration technique (FIT) has been introduced to solve Maxwell's equations for six-component fields on a finite region of space. It presents a numerical solution of Maxwell's equations and uses a differential formulation of Maxwell's equations adopting the finite difference method [14]. From the above analysis, it can be ascertained that the FIT method has been applied in analyzing antennas and antenna arrays. One of these procedures is where Maxwell's equations are solved employing the finite element method. The aforementioned technique, which is derived from FEM and used to model and analyze antenna structures and surrounding fields, is useful for evaluating complicated antenna structures and gives the theoretical framework for using numerical solutions [15]. Computer Simulation Technology (CST) Microwave Studio – this is an electromagnetic simulation software package used in the engineering field. A detailed study of feed lengths that are likely to determine the performance of the microstrip patch antennas has been done [16]. This paper aims at analyzing the performances as well as designing techniques of the antennas commonly used in high-frequency 5G communication technology [17]. This paper focuses on the analysis of the effect of feed length on the microstrip patch antennas and how that may affect their efficiency. Generally, an antenna feed length longer than the current half-wavelength adds more current at each turn in the magnetic loop, thus enhancing the effectiveness of the antenna

as compared to shorter feed lengths that decrease the efficiency of the antenna. These results support the assertion that the feed length is a factor among the larger considerations in the design of microstrip patch antennas [18].

In this study, a microstrip patch antenna of rectangular shape is designed at 28 GHz with various conductor thicknesses, but having the same geometrical parameters and with various feed lengths of the antenna in the 20-36 GHz for 5G wireless communication systems in the CST environment. As observed from the previous simulation results where graphical representations of the three materials used for patch conductors are presented, it is clear that the three materials match the desired operating frequency and operating potential. On analyzing the above graphs based on the return loss (S11), it is also found that all the conductors used here provide the optimum results at the feed length of 1.05 mm. It was seen that return loss depends on conductor type and the best conductor was aluminum, gold and copper.

The rest of the paper is composed of the following sections. In section 2, improving upon the propagation characteristics of signals through microstrip patch antennas is demonstrated by simulating sophisticated electromagnetic fields by FIT. First, it discusses the theory that is relevant to the microstrip patch antenna design. In section 3, the design and simulation of rectangular microstrip patch antenna for wireless communication is described. Thus, the roles of the mentioned 5G antenna parameters of S11, voltage standing wave ratio, bandwidth (BW), gain, and directivity in CST simulation are analyzed in the antenna for various conductor patches and feed lengths in the range of 20-36 GHz with the operating resonance at 28 GHz. Based on the simulation results in section 4, the best conductor patch and the optimal feed length are presented.

## 2. Microstrip Patch Antenna (MPA) Design

The differential formulation of Maxwell's equations can be solved by the FIT. FIT employs something called finite integration as the mechanism for analyzing the behavior of electromagnetic fields. As suggested by its name, FIT is an efficient method of taking a limited number of measurements of the strengths of the electromagnetic fields and computing the measured fields. Using the finite difference method, the derivatives of the fields are approximated in a numerical form, and in this manner, a numerical solution to Maxwell's equation is derived. This method is applied where the real situations of electric and magnetic fields are desired and in the resolution of high precision such as lithography [19].

The microstrip antenna is made of an upper metal strip as its top layer. This is a thin strip of metal that provides the primary framework of the antenna, and its function is to code and send electromagnetic waves. They are generally formed of conductive materials. A link that connects various parts of a single software program or a related group of programs is also referred to as a patch. The middle layer is made of a dielectric material whereas the top layer is made of a conductor material called metal. The interlayer affects the electrical characteristics of the antennas and assists in their operating efficiency. The lowest layer of the radiating system in the case of transmitting antennas is a substrate or a reflective surface placed under the antenna. This layer gives directed radiation and enhances the ability of the antenna in its operation [20]. In the design process of microstrip patch antennas for 5G/B5G (beyond fifth generation) applications, performance criteria such as frequency, bandwidth, gain and directivity has been evaluated. These criteria affect the antenna performance to be used in 5G/B5G applications [21]. Modular antenna arrays designed in the 5G field have been shown to have high performance in real-world applications in terms of antenna performance, cost-effectiveness, scalability and application [22]. The simplest kind of microstrip patch antenna is illustrated in Figure 1.

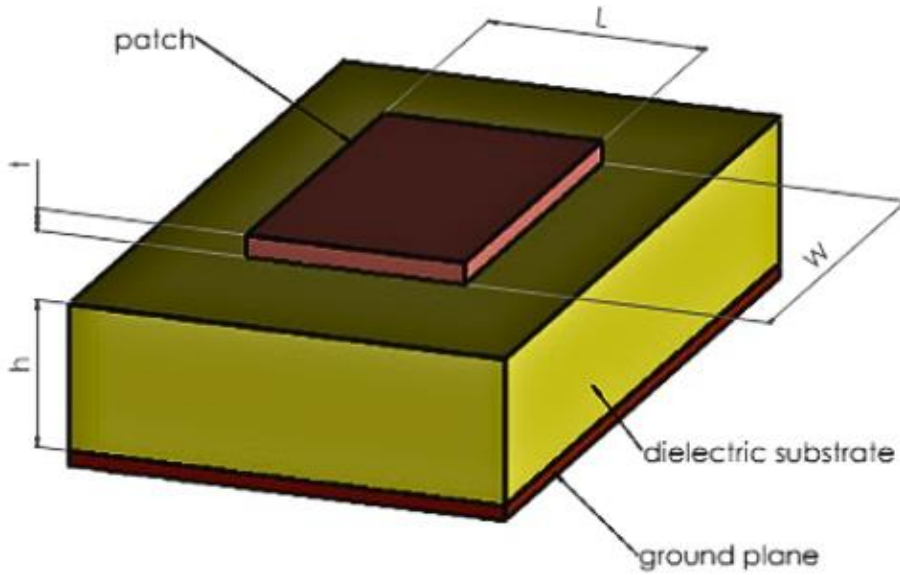


Fig. 1. Microstrip patch antenna structure.

In the operation of microstrip antennas, achieving optimal performance requires careful selection and placement of the feed point and SMA port to facilitate efficient reception and transmission of RF signals by the antenna. In this investigation, a 50-ohm SMA port serves as the feed interface. The feed structure for the microstrip patch antenna is shown in Figure 2.

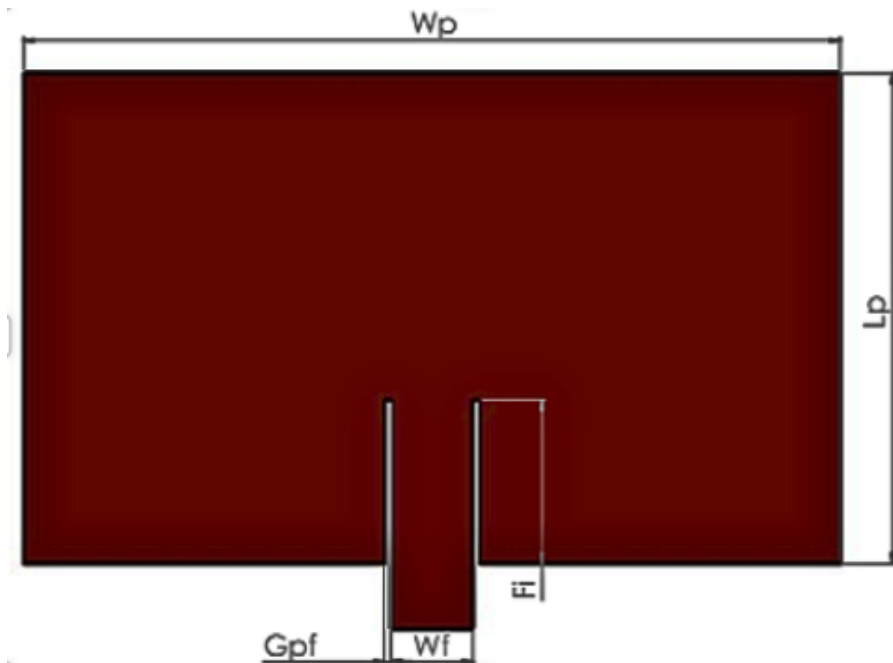


Fig. 2. Microstrip patch structure with patch feed.

A microstrip patch structure is used with a patch feed. The width (W) and length (L) of the antenna patch are determined using Equation (1);

$$W = \frac{c}{2f \sqrt{\epsilon_r + 1}} . \quad (1)$$

To calculate the length ( $L_{eff}$ ), we first determine the dielectric constant ( $\epsilon_{reff}$ ) from the Equation (3) and substitute it into Equation (2);

$$L = \frac{c}{2f \sqrt{\epsilon_{eff}}} . \quad (2)$$

The effective dielectric constant is determined using the formula in Equation (3);

$$\epsilon_{eff} = \frac{\epsilon_r + 1}{2} + \frac{\epsilon_r - 1}{2} \left(1 + 12 \frac{h}{w}\right)^{-1/2} . \quad (3)$$

The total length is derived using the following formula;

$$\Delta L = 0.412 \frac{(\epsilon_{eff} + 0.3) \left(\frac{w}{h} + 0.264\right)}{(\epsilon_{eff} - 0.258) \left(\frac{w}{h} - 0.8\right)} . \quad (4)$$

The length extension ( $\Delta L$ ) is calculated as;

$$\Delta L = L_{eff} - 2 \Delta L . \quad (5)$$

The length of the inner part can be determined through the formula defined as [23];

$$F_i = \frac{6h_s}{2} . \quad (6)$$

### 3. Antenna Design and Analysis for 5G & Beyond Wireless Communication

The objective of this research is to present an innovative microstrip antenna for 5G wireless networks that offer better radiation characteristics and is convenient in terms of dimension and mechanical stability. Thus, defining 28 GHz as a resonant frequency in this study. Rogers5880 is employed for dielectric layer material. The layer thickness of can be noted that for H = 0.2 mm and the dielectric constant  $\epsilon_r = 2.2$ . From the resonance frequency equations, the respective dimensions of the WP and LP antennas are found, and patch size is calculated as 4.4 mm and 3.44 mm, respectively. The ground plane dimensions are WG= 5.6 mm and LG=4.65 mm. The proposed internal feed length is calculated using Equations (1)-(6). The feed length F=1.05 mm, the feed length width WF=0.6 mm, the gap between the patch and the feed line G=0.1 mm. The design of the antenna structure presented in this work with the help of CST is shown in Figure 3.

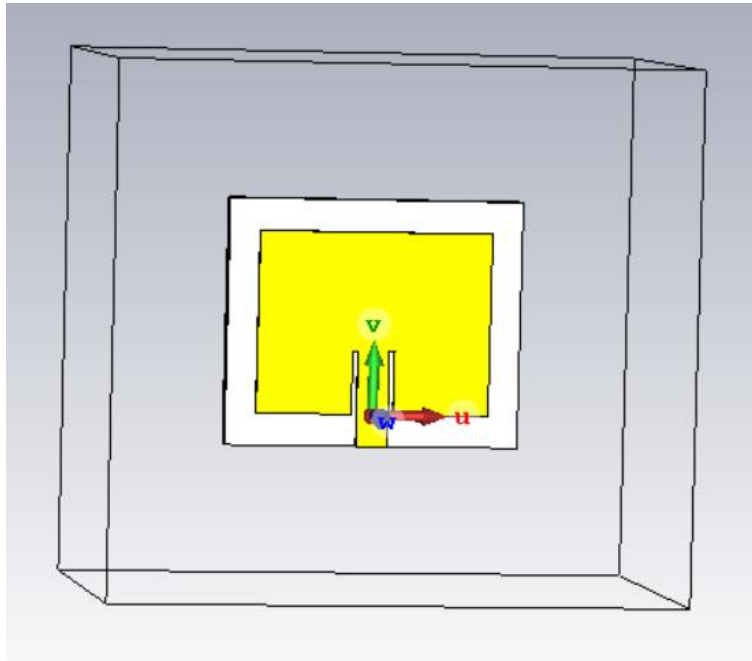


Fig. 3. Structure of the designed antennas.

The antenna dimensions used for the rectangular patch microstrip antenna design are shown in Table 1.

Table 1. Design parameters and dimensions of the proposed antenna.

Parameters	Definition	Value (mm)
WG	Floor and Surface Width	5.60
LG	Floor and Surface Length	4.65
WP	Patch Width	4.40
LP	Patch Length	3.44
H	Thickness of the substrate	0.20
MT	Patch thickness	0.035
Gpf	Gap between patch and feed line	0.10
Fi	Inner feed length	1.05
WF	Microstrip line feed width	0.60

The antenna designs utilize copper, aluminum and gold conductors in their construction. The measurements for S11, VSWR, BW and antenna radiation patterns are conducted for each conductor type across nine feed lengths using the calculated patch antenna dimensions.

The return loss graphs for the copper, gold, and aluminum conductors are shown respectively in Figure 4, 5 and 6.

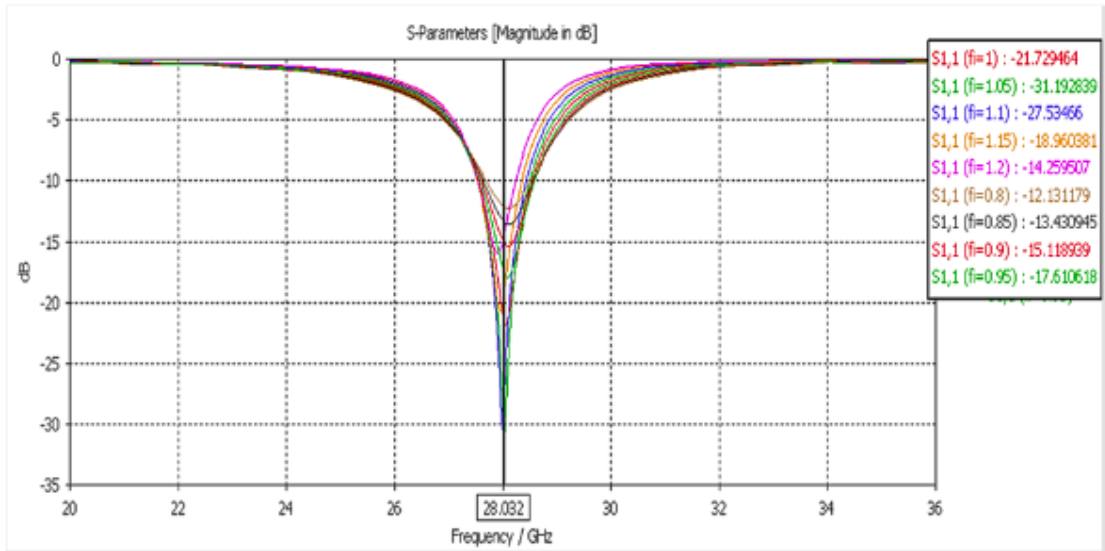


Fig. 4. Return loss for the copper conductor.

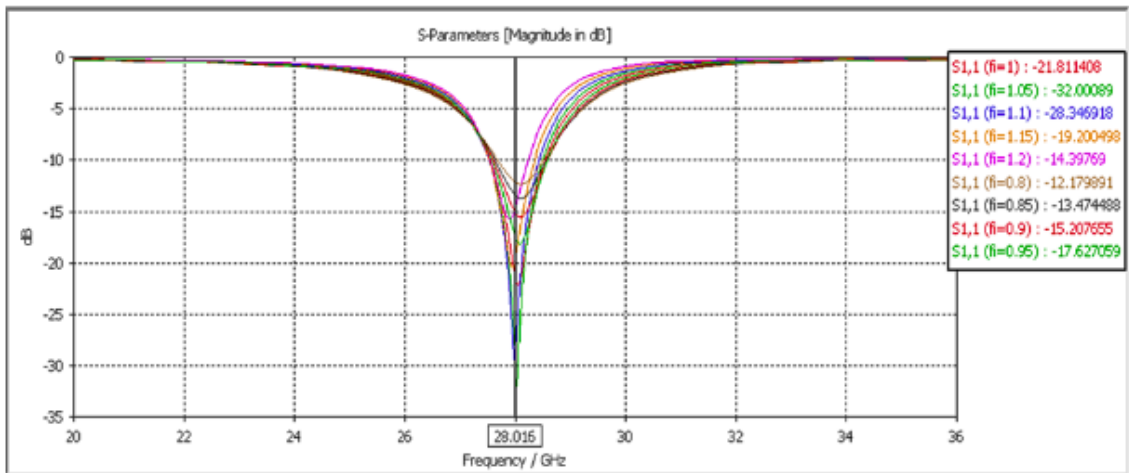


Fig. 5. Return loss for the gold conductor.

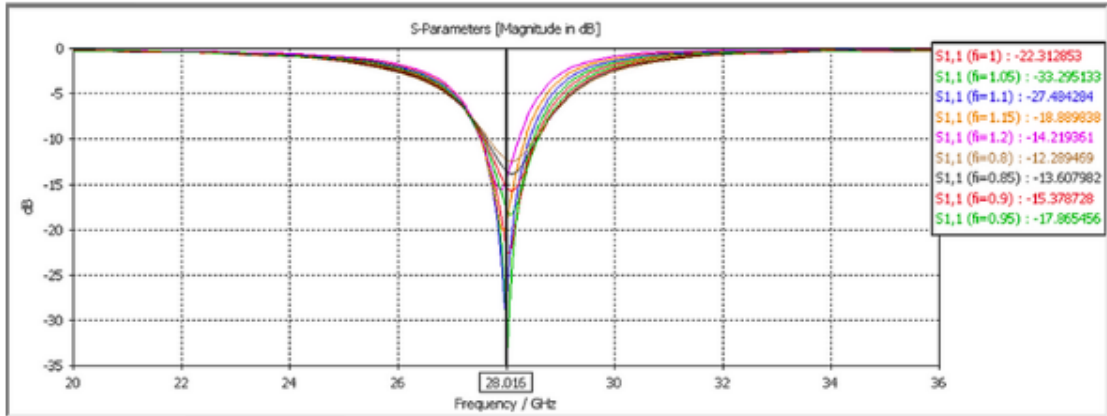


Fig. 6. Return loss for the aluminum conductor.

VSWR is a critical parameter indicating voltage variations along the transmission line. The graphs illustrating VSWR are presented in Figures 7-9.

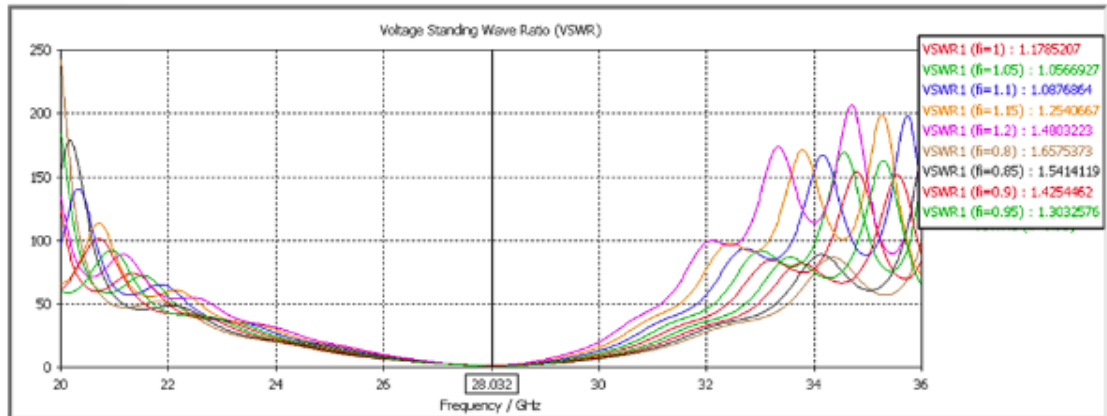


Fig. 7. VSWRs for the copper conductor at nine different feed lengths.

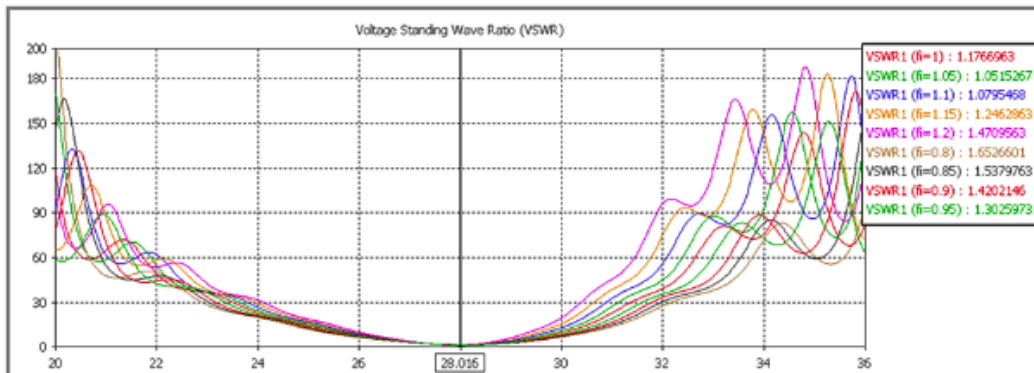


Fig. 8 VSWRs for the gold conductor at nine different feed lengths.

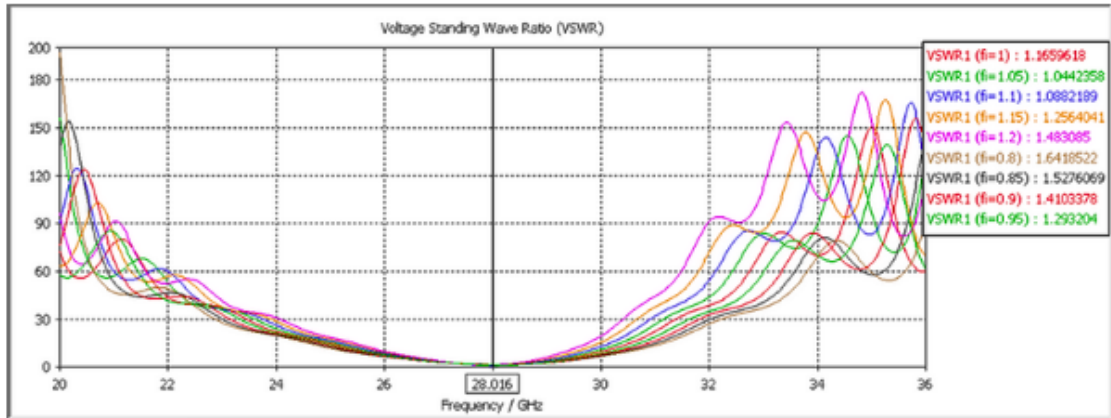


Fig. 9 VSWRs for the aluminum conductor at nine different feed lengths.

S11, VSWR, Frequency (Fr) and BW values for three different conductors at nine different feed lengths are shown in Table 2.

Table 2. S11, VSWR and BW values of different conductor antennas for different feed lengths.

Conductor Material	Inner feed length	S11(dB)	VSWR	Fr (GHz)	BW (MHz)
Copper	fi:0.8mm	-12.13	1.65	28.03	814
	fi:0.85mm	-13.43	1.54	28.03	950
	fi:0.9mm	-5.11	1.42	28.03	973
	fi:0.95mm	-17.61	1.30	28.03	1002
	fi: 1mm	-21.72	1.17	28.03	996
	fi:1.05mm	-31.19	1.05	28.03	968
	fi:1.1mm	-27.53	1.08	28.03	908
	fi:1.15mm	-18.96	1.25	28.03	820
	fi:1.2mm	-14.25	1.48	28.03	693
Gold	fi:0.8mm	-12.17	1.65	28.01	828
	fi:0.85mm	-13.47	1.53	28.01	927
	fi:0.9mm	-15.20	1.42	28.01	987
	fi:0.95mm	-17.62	1.30	28.01	1018
	fi: 1mm	-21.81	1.17	28.01	1002
	fi:1.05mm	-32.00	1.05	28.01	972
	fi:1.1mm	-28.34	1.07	28.01	910
	fi:1.15mm	-19.20	1.24	28.01	820
	fi:1.2mm	-14.39	1.47	28.01	692
Aluminum	fi:0.8mm	-12.28	1.64	28.01	843
	fi:0.85mm	-13.60	1.52	28.01	939
	fi:0.9mm	-15.37	1.41	28.01	996
	fi:0.95mm	-17.86	1.29	28.01	1017
	fi: 1mm	-22.31	1.16	28.01	991
	fi:1.05mm	-33.29	1.04	28.01	976
	fi:1.1mm	-27.48	1.08	28.01	914
	fi:1.15mm	-18.88	1.25	28.01	822
	fi:1.2mm	-14.21	1.48	28.01	690

In Table 2 we observe that, for a feed length (Fi) of 0.8 mm the resonance frequency of the microstrip patch antenna with copper conductor is 28.03 GHz, with a S11 of -12.13 dB a VSWR value of 1.65 and a BW of 814 MHz. The resonance frequency for the antenna with the gold conductor is slightly lower at 28.01 GHz with an S11 value of -12.17 dB VSWR value of 1.65 and bandwidth of 828 MHz. Similarly, the microstrip patch antenna with aluminum conductor also resonates at around 28.01 GHz with an S11 value of -12.28 dB VSWR value at 1.64 and BW reaching up to 843 MHz.

For a feed length ( $F_i$ ) increased to 0.85 mm, the S11 varies as follows: for the copper conductor, it is -13.43 dB with a VSWR of 1.54 and a bandwidth of 950 MHz; for the gold conductor, it is -13.47 dB with a VSWR of 1.53 and a bandwidth of 927 MHz; and for the aluminum conductor, it reaches -13.60 dB with a VSWR of 1.52 and a bandwidth of 939 MHz.

When the feed length is 0.9 mm, for the copper conductor microstrip patch antenna the S11 is -5.11 dB with a VSWR of 1.42 and a BW of 973 MHz. For the gold conductor microstrip patch antenna, the S11 is -15.20 dB with a VSWR value of 1.42 and a BW of 987 MHz. Meanwhile, for the aluminum conductor microstrip patch antenna the S11 is -15.37 dB with a VSWR of 1.41, and a BW of 996 MHz.

As shown in Table 2, this is at the feedlength of 0.95 mm, the copper conductor microstrip patch antenna gain an attractive S11 value at -17.61 dB with VSWR value of 1.30. BW at 1002 MHz. The S11 value at -17.62 dB, VSWR at 1.30 and BW at 1018 MHz obtained for the gold conductor microstrip patch antenna The S11 value of the aluminum-conductor microstrip patch antenna is -17.86 dB, the VSWR value is 1.29, and the bandwidth is 1017 MHz.

The S11, VSWR, and BW are -21.72 dB, 1.17 and 996 MHz, respectively, for the copper conductor microstrip patch antenna when the feed length is 1 mm. For the gold conductor variant, the S11 value is -21.81 dB, with a VSWR of 1.17 and a bandwidth BW of 1002 MHz. An aluminum conductor microstrip patch antenna has S11=-22.31 dB, VSWR=1.16, and BW=991 MHz.

The S11 of the copper conductor microstrip patch antenna, for a feed length of 1.05 mm, is -31.19 dB, with a VSWR of 1.05, and the proposed antenna has a BW of 968 MHz. The gold conductor version returned an S11 of -32 dB VSWR 1.05 up to 972 MHz, while the aluminum conductor type has an S11 of -33.29 dB VSWR 1.04 with BW reaching approximately 976 MHz.

With the feed length set to be at 1.1 mm, observations for the copper conductor microstrip patch antenna include an S11 reading of around -27.53 dB along with a VSWR value about 1.08 within a BW that reaches up to, around approximately 908 MHz. The gold conductor microstrip patch antenna has an S11 value of -28.34 dB a VSWR value of 1.07 and a BW of 910 MHz. For the aluminum conductor microstrip patch antenna, the S11 value is -27.48 dB the VSWR value is 1.08. The BW is 914 MHz.

When the  $F_i$  measures 1.15 mm, the copper conductor microstrip patch antenna exhibits an S11 value of -18.96 dB a VSWR value of 1.25, and a BW of 908 MHz. In comparison for the gold conductor microstrip patch antenna at this feed length, we observe an S11value of -19.20 dB with a VSWR of 1.24 and a BW of 820 MHz; while for the aluminum conductor version, it is depicted that the S11 value of 18.88 dB with a VSWR of 1.25 and a BW of 822 MHz.

With a feed length set at 1.2 mm, the copper conductor microstrip patch antenna exhibits an S11 value of -14.25 dB alongside a VSWR value of 1.48 and a BW spanning 693 MHz. The gold conductor microstrip patch antenna records a S11 value at -14.39 dB with a VSWR value of 1.47 and BW reaching up to 692 MHz; similarly, the aluminum conductor variant showcases a S11 reading at -14.21 dB with a VSWR figure of 1.48 and BW capped at 690 MHz.

The path of the antenna radiation is a mathematical description of antenna radiation fields in the long-range direction at different spatial positions. This model helps in evaluating the nature of density of the radiated power of the antenna and details the emission from the antenna at great distances of the electromagnetic waves. The antenna selection model is determined by factors such as the antenna dimensions, operating frequency, and the feeding techniques and influence of the environment. Thus, the antenna radiation pattern is used for the assessment of the performance and efficiency of the antenna in the communication system and constitutes an important element of a communication system. The conductor cross-sectional representations from three distinct current-carrying forms are presented in Figures 10-12.

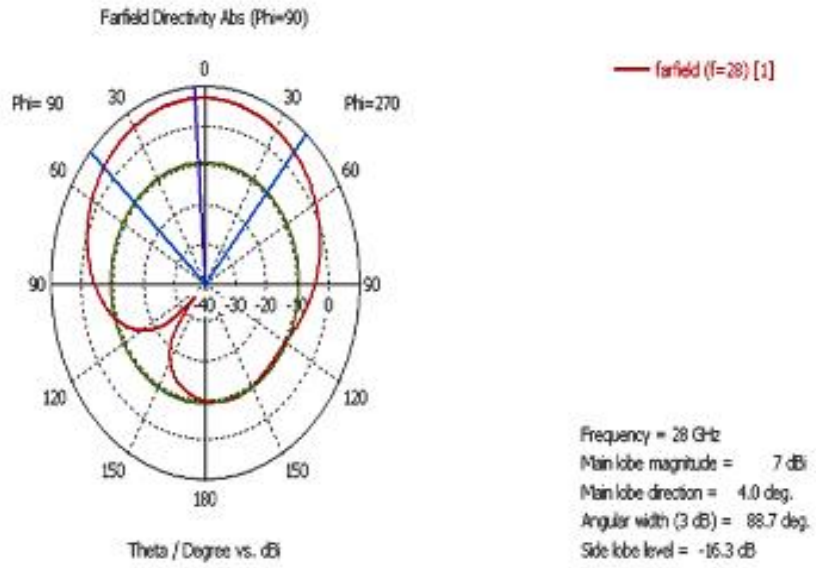


Fig. 10. 2D antenna radiation pattern for the copper conductor.

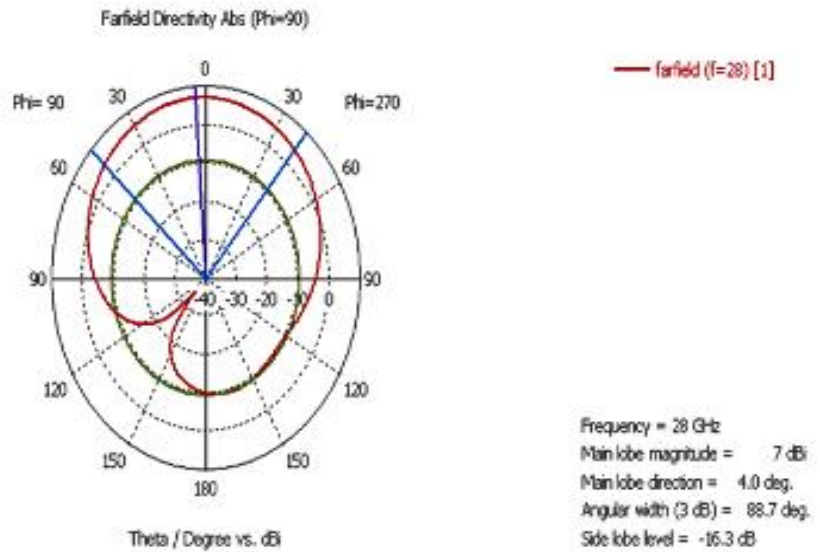


Fig. 11. 2D antenna radiation pattern for the gold conductor.

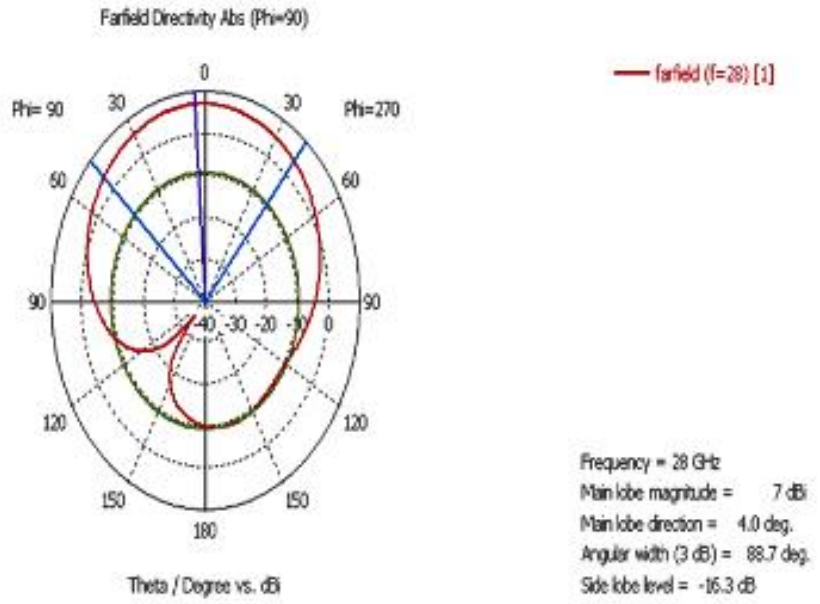


Fig. 12. 2D antenna radiation pattern for the aluminum conductor.

The three-dimensional (3D) directivity representation of the antennas design can be seen in Figure 13-15.

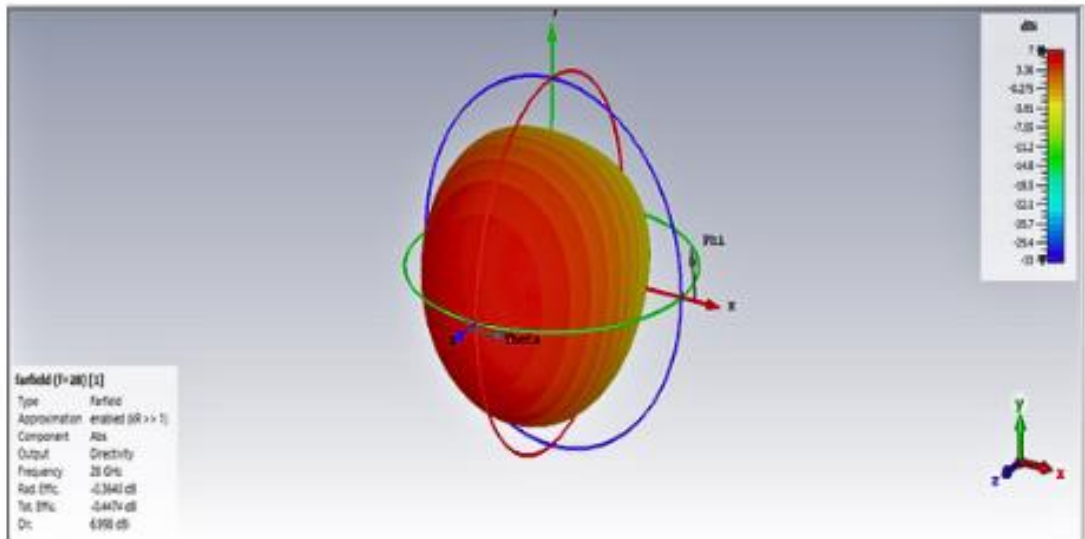


Fig. 13. 3D directivity pattern of the copper conductor antenna.

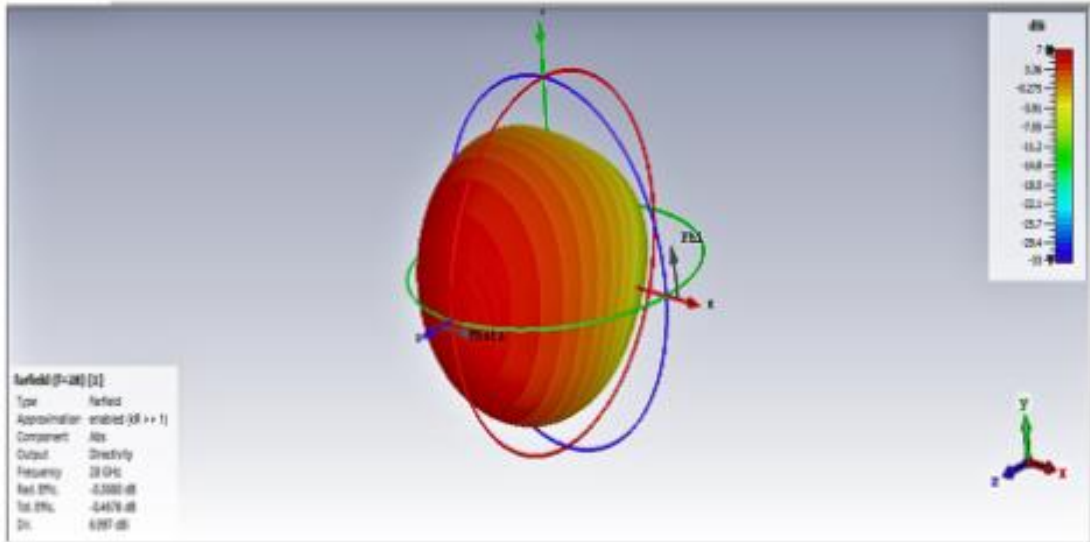


Fig. 14. 3D directivity pattern of the gold conductor antenna.

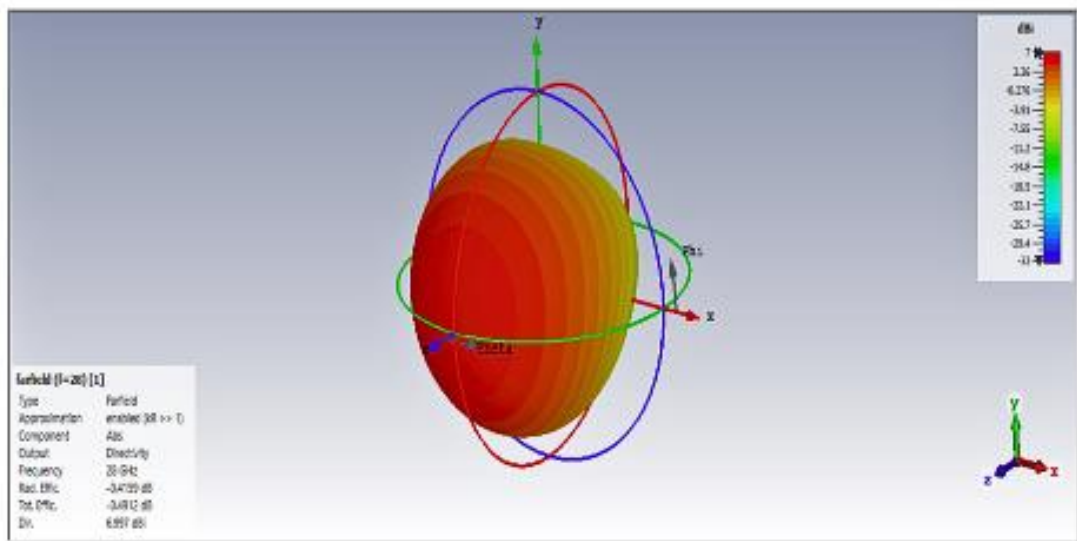


Fig. 15. 3D directivity pattern of the aluminum conductor antenna.

The maximum directivity values in their three representations are approximately at about 6.99 dBi for copper conductor, gold conductor and aluminum conductor antennas.

Additionally, Figures 16-18 exhibits three-dimensional representations of gain patterns, for these antennas.

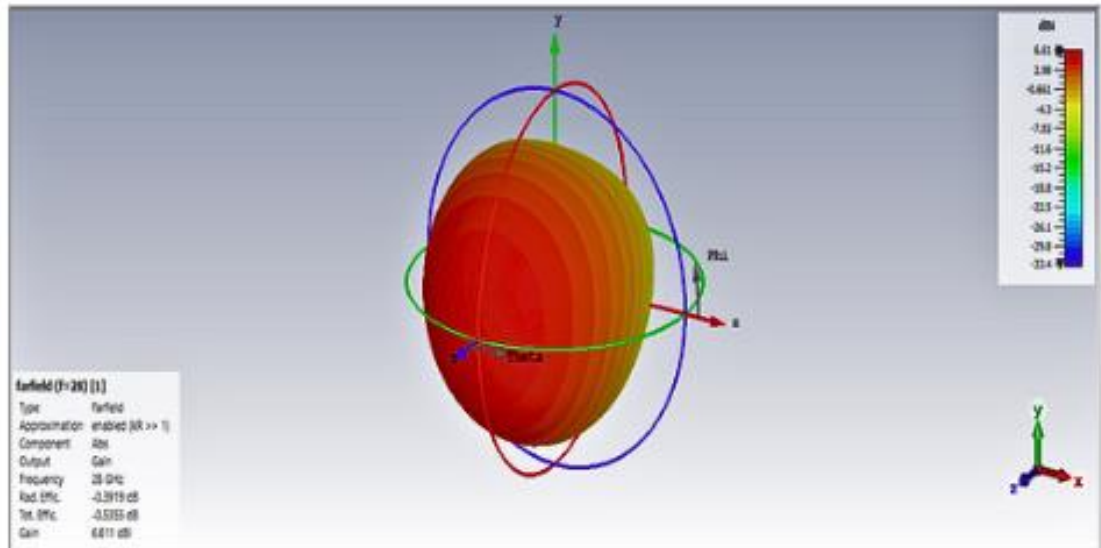


Fig. 16. 3D gain pattern of the copper conductor antenna.

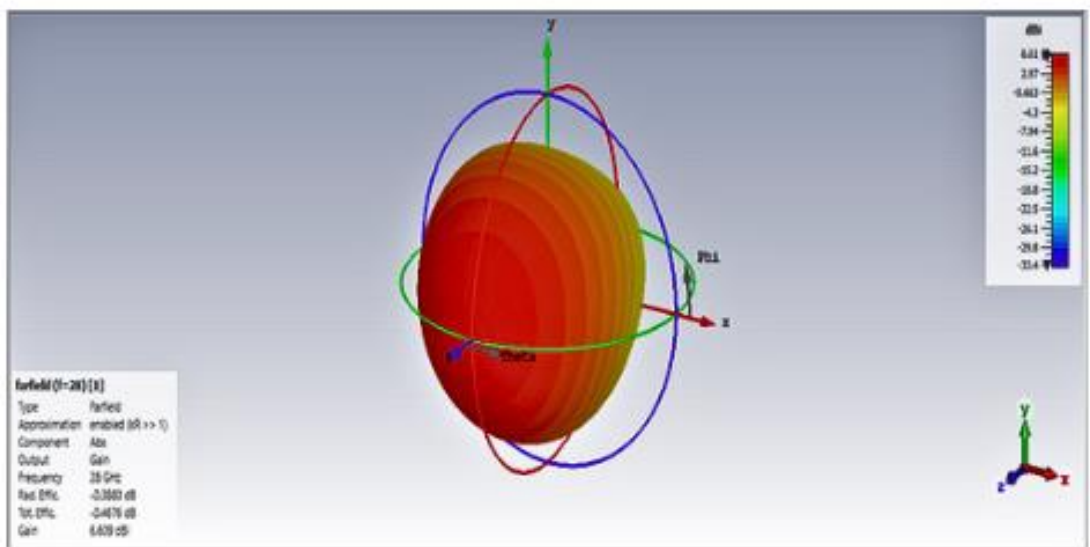


Fig. 17. 3D gain pattern of the gold conductor antenna.

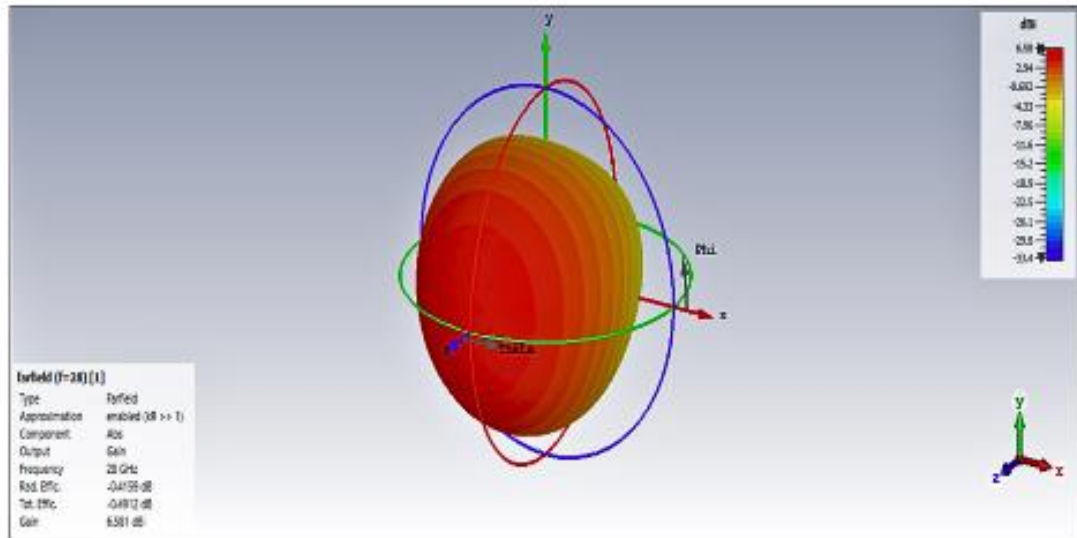


Fig. 18. 3D gain pattern of the aluminum conductor antenna.

The maximum gain values of the 3D representation for the copper-conductor, gold-conductor and aluminum-conductor antennas are 6.61, 6.60 and 6.58 dBi, respectively.

#### 4. Conclusions

In this study, a microstrip patch antenna of rectangular shape is designed at 28 GHz with various conductor thicknesses but having the same geometrical parameters and with various feed lengths of the antenna in the 20-32 GHz for 5G wireless communication systems in the CST environment. As observed from the previous simulation results where graphical representations of the three materials used for patch conductors are presented, it is clear that the three materials dovetails into the desired operating frequency and operating potential. On analyzing the above graphs based on the return loss, it is also found that all the conductors used here provide the optimum results at the feed length of 1.05 mm. It was observed that the return loss varies with the type of conductor, with aluminum being the most effective, followed by gold and copper.

There is much influence of the various types of conductors used on the material of the antenna patch and the feed lengths used in microstrip patch antenna based on the findings of this study. We determined that a feed length of 1.05 mm yields the optimal return loss compared to the three conductor types assessed in this study. For the copper conductor, they were able to attain a return loss of -31.19 dB at a resonant frequency of 28.03 GHz and BW 968 MHz. The gold conductor is slightly better at a center frequency of about 28.01 GHz obtaining a S11 of -32 dB and a bandwidth of 972 MHz. However, the aluminum conductor achieved the superior S11 of -33.29 dB at the same resonant frequency 28.01 GHz with the greatest BW 976 MHz among all three conductors. Fortunately, the analysis results show that at the respective resonant frequencies of the three conductors, the VSWR level remains at the low value of 1.05. A VSWR of 2 or less indicates high efficiency in antenna operation. Based on these findings, microstrip patch antennas with optimized feed lengths and various conductors are expected to exhibit improved radiation characteristics suitable for 5G applications.

#### Acknowledgements

All authors declare that there is no conflict of interest regarding the publication of this article. In addition, this research received no specific grant from any funding agency in the public, commercial, or non-profit organizations.

## References

- [1] M. Shafi, A. Hashimoto, M. Umehira, S. Ogoose, and T. Murase, "Wireless communications in the twenty-first century: A perspective," *Proc. IEEE*, vol. 85, no. 10, pp. 1622-1638, Oct. 1997, doi: 10.1109/5.640770.
- [2] S. Kumar, "Mobile communications: Global trends in the 21st century," *Int. J. Mobile Commun.*, vol. 2, no. 1, pp. 67-86, 2005, doi: 10.1504/IJMC.2004.004488.
- [3] J. Pizarov and G. Mester, "The impact of 5G technology on life in the 21st century," *IPSI Trans. Adv. Res.*, vol. 16, no. 2, pp. 11-14, 2020.
- [4] I. Umakoglu, M. Namdar, and A. Basgumus, "UAV-Assisted Cooperative NOMA System with the  $n$ th Best Relay Selection," *Adv. Electr. Comput. Eng.*, vol. 23, no. 3, pp. 39-46, 2023, doi: 10.4316/AECE.2023.03005.
- [5] I. Umakoglu, M. Namdar, and A. Basgumus, "Performance Evaluation of OTFS-NOMA Scheme for High Mobility Users," *Sakarya Univ. J. Comput. Inf. Sci.*, vol. 6, no. 3, pp. 253-260, 2023, doi: 10.35377/saucis...1391813.
- [6] I. Umakoglu, M. Namdar and A. Basgumus, "Deep Learning-Assisted Signal Detection for OTFS-NOMA Systems," *IEEE Access*, pp. 1-11, doi: 10.1109/ACCESS.2024.3449812.
- [7] M. Namdar, A. Guney, F. K. Bardak, and A. Basgumus, "Ergodic Capacity Estimation with Artificial Neural Networks in NOMA-based Cognitive Radio Systems," *Springer Arab. J. Sci. Eng.*, vol. 49, pp. 6459-6468, 2024, doi: 10.1007/s13369-023-08279-6.
- [8] A. Basgumus, F. Kocak, and M. Namdar, "BER Performance Analysis for Downlink NOMA Systems over Cascaded Nakagami-m Fading Channels," *Springer Ann. Telecommun.*, vol. 79, pp. 447-453, 2024, doi: 10.1007/s12243-023-01002-4.
- [9] S. K. Ezzulddin, S. O. Hasan, and M. M. Ameen, "Microstrip patch antenna design, simulation and fabrication for 5G applications," *Simul. Model. Pract. Theory*, vol. 116, p. 102497, 2022, doi: 10.1016/j.simpat.2022.102497.
- [10] P. Balachandran, A. Nidadavolu, O. P. Kumar, S. Vincent, and T. Ali, "A Microstrip Patch Antenna with Enhanced Bandwidth for Millimeter Wave 5G Application," *J. Phys.: Conf. Ser.*, vol. 1706, no. 1, p. 012101, 2020, doi:10.1088/1742-6596/1706/1/012101.
- [11] B. Tutuncu, "Microstrip Antenna for 5G Communication: Design and Performance Analysis," in Proc. 2020 Int. Congr. Human-Comput. Interact., *Optim. Robot. Appl. (HORA)*, 2020, pp. 1-4, doi: 10.1109/HORA49412.2020.9152855.
- [12] P. Elliot, "The applied computational electromagnetics society," *IEEE Antennas Propag. Mag.*, vol. 33, no. 1, pp. 18-19, 1991, doi: 10.1109/74.80657.
- [13] M. N. Sadiku, *Elements of Electromagnetics*, 4th ed., Oxford Univ. Press, 2009.
- [14] T. Weiland, "A discretization model for the solution of Maxwell's equations for six-component fields," *Arch. Elektron. Uebertragungstechn.*, vol. 31, pp. 116-120, 1977.
- [15] M. J. Jian and J. R. Douglas, *Finite Element Analysis of Antennas and Arrays*, John Wiley & Sons, Inc., 2009.
- [16] T. S. Aina, O. O. Akinte, and B. A. Iyaomolere, "Investigation on performance of microstrip patch antenna for a practical wireless local area network (WLAN) application," *Int. J. Res. Appl. Sci. Eng. Technol. (IJRASET)*, vol. 10, no. 1, pp. 221-226, 2022, doi: 10.22214/ijraset.2022.39799.
- [17] M. Khasiyev, "28 GHz frekansında 5G kablosuz haberleşme için S-şekilli mikroşerit anten tasarımı ve analizi," Yüksek Lisans Tezi, Bursa Uludağ Üniversitesi, 2023.
- [18] H. M. Bhatt, "Study on the effect of inset feed length on radiation characteristic of rectangular microstrip patch antenna," in S. Lathigara, H. M. Bhatt, and V. Unadkat (Eds.), *Proc. Natl. Conf. Emerg. Trends Comput., Electr. Electron. (ETCEE-2015)*, Rajkot, 2015.
- [19] R. Zhabiz, *The Finite Integration Technique (FIT) and the Application in Lithography Simulations*, Friedrich-Alexander Univ., 2011.
- [20] C. A. Balanis, *Antenna Theory: Analysis and Design*, John Wiley & Sons Ltd., 2016.
- [21] H. Attar, R. S. Agieb, A. Amer, A. Solyman, and M. S. Aziz, "Microstrip Patch Antenna Design and Implementation for 5G/B5G Applications", *2022 International Engineering Conference on Electrical, Energy, and Artificial Intelligence (EICEEAI)*, Zarqa, Jordan, 2022, pp. 1-6, doi: 10.1109/EICEEAI56378.2022.10050499.
- [22] A. Ashraff, T. Gunawan, M. Kartiwi, L. Nur, B. Nurgoho and R. Astuti, "Advancements and Challenges in Scalable Modular Antenna Arrays for 5G Massive MIMO Networks", *IEEE Access*, vol. 12, pp. 57895 - 57916, doi: 10.1109/ACCESS.2024.3391945.
- [23] A. S. Chaurasia, A. K. Shankhwar and A. Singh, "Design of Novel Patch Antenna using CST Software," *2021 Second International Conference on Electronics and Sustainable Commun. Systems (ICESC)*, 2021, pp. 586-591, doi: 10.1109/ICESC51422.2021.9532843.